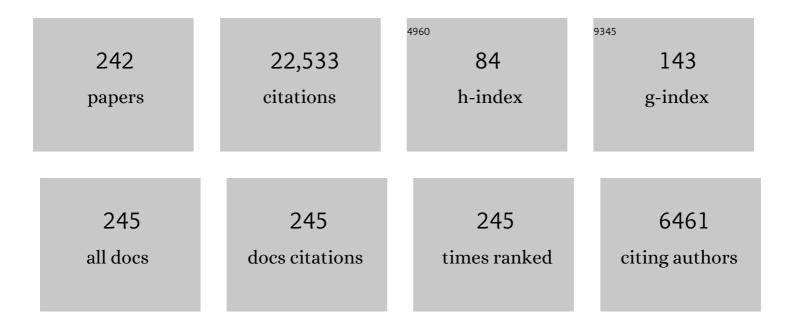
Scott L Murchie

List of Publications by Year in descending order

Source: https://exaly.com/author-pdf/3169616/publications.pdf Version: 2024-02-01



#	Article	IF	CITATIONS
1	Science Goals and Mission Concept for a Landed Investigation of Mercury. Planetary Science Journal, 2022, 3, 68.	3.6	2
2	Maximizing the Science and Resource Mapping Potential of Orbital VSWIR Spectral Measurements of Mars. , 2021, 53, .		0
3	The Mars Orbiter for Resources, Ices, and Environments (MORIE) Science Goals and Instrument Trades in Radar, Imaging, and Spectroscopy. Planetary Science Journal, 2021, 2, 76.	3.6	2
4	Anomalous Phyllosilicateâ€Bearing Outcrops South of Coprates Chasma: A Study of Possible Emplacement Mechanisms. Journal of Geophysical Research E: Planets, 2020, 125, e2019JE006043.	3.6	5
5	A search for early- to mid-Noachian chloride-rich deposits on Mars. Icarus, 2020, 338, 113552.	2.5	5
6	Multiple mineral horizons in layered outcrops at Mawrth Vallis, Mars, signify changing geochemical environments on early Mars. Icarus, 2020, 341, 113634.	2.5	24
7	Composition of Amazonian volcanic materials in Tharsis and Elysium, Mars, from MRO/CRISM reflectance spectra. Icarus, 2019, 328, 274-286.	2.5	27
8	The distribution, composition, and particle properties of Mars mesospheric aerosols: An analysis of CRISM visible/near-IR limb spectra with context from near-coincident MCS and MARCI observations. Icarus, 2019, 328, 246-273.	2.5	40
9	Measuring the Elemental Composition of Phobos: The Marsâ€moon Exploration with GAmma rays and NEutrons (MEGANE) Investigation for the Martian Moons eXploration (MMX) Mission. Earth and Space Science, 2019, 6, 2605-2623.	2.6	26
10	Spectral Analyses of Mercury. , 2019, , 351-367.		0
11	Visible to Short-Wave Infrared Spectral Analyses of Mars from Orbit Using CRISM and OMEGA. , 2019, , 453-483.		6
12	Global Distribution and Spectral Properties of Lowâ€Reflectance Material on Mercury. Geophysical Research Letters, 2018, 45, 2945-2953.	4.0	41
13	Challenges in the Search for Perchlorate and Other Hydrated Minerals With 2.1â€Ĥ⁄4m Absorptions on Mars. Geophysical Research Letters, 2018, 45, 12180-12189.	4.0	40
14	Spectral Reflectance Constraints on the Composition and Evolution of Mercury's Surface. , 2018, , 191-216.		9
15	Mercury's Hollows. , 2018, , 324-345.		12
16	Calibration, Projection, and Final Image Products of MESSENGER's Mercury Dual Imaging System. Space Science Reviews, 2018, 214, 1.	8.1	53
17	Overview of Phobos/Deimos Regolith Ion Sample Mission (PRISM) concept. , 2018, , .		1
18	The structural, stratigraphic, and paleoenvironmental record exposed on the rim and walls of Iazu Crater, Mars. Journal of Geophysical Research E: Planets, 2017, 122, 1138-1156.	3.6	6

#	Article	IF	CITATIONS
19	Vertical profiles of Mars 1.27µm O 2 dayglow from MRO CRISM limb spectra: Seasonal/global behaviors, comparisons to LMDGCM simulations, and a global definition for Mars water vapor profiles. Icarus, 2017, 293, 132-156.	2.5	58
20	Extending MESSENGER's Mercury dual imager's eight-color photometric standardization to cover all eleven filters. Icarus, 2017, 297, 83-89.	2.5	3
21	Compositional and structural constraints on the geologic history of eastern Tharsis Rise, Mars. Icarus, 2017, 284, 43-58.	2.5	40
22	Discovery of alunite in Cross crater, Terra Sirenum, Mars: Evidence for acidic, sulfurous waters. American Mineralogist, 2016, 101, 1527-1542.	1.9	51
23	Evidence from MESSENGER for sulfur―and carbonâ€driven explosive volcanism on Mercury. Geophysical Research Letters, 2016, 43, 3653-3661.	4.0	57
24	Mars-Moons Exploration, Reconnaissance, and Landed Investigation (MERLIN). , 2016, , .		1
25	New insights into gully formation on Mars: Constraints from composition as seen by MRO/CRISM. Geophysical Research Letters, 2016, 43, 8893-8902.	4.0	21
26	Analysis of MESSENGER highâ€resolution images of Mercury's hollows and implications for hollow formation. Journal of Geophysical Research E: Planets, 2016, 121, 1798-1813.	3.6	30
27	Determining shape of a seasonally shadowed asteroid using stellar occultation imaging. Planetary and Space Science, 2016, 131, 24-32.	1.7	0
28	Smectite deposits in Marathon Valley, Endeavour Crater, Mars, identified using CRISM hyperspectral reflectance data. Geophysical Research Letters, 2016, 43, 4885-4892.	4.0	39
29	Methodology for finding and evaluating safe landing sites on small bodies. Planetary and Space Science, 2016, 134, 71-81.	1.7	8
30	Imaging Mercury's polar deposits during MESSENGER's lowâ€altitude campaign. Geophysical Research Letters, 2016, 43, 9461-9468.	4.0	31
31	Mineralogical indicators of Mercury's hollows composition in MESSENGER color observations. Geophysical Research Letters, 2016, 43, 1450-1456.	4.0	42
32	Orbital evidence for more widespread carbonateâ€bearing rocks on Mars. Journal of Geophysical Research E: Planets, 2016, 121, 652-677.	3.6	109
33	Application of multiple photometric models to disk-resolved measurements of Mercury's surface: Insights into Mercury's regolith characteristics. Icarus, 2016, 268, 172-203.	2.5	40
34	Remote sensing evidence for an ancient carbon-bearing crust on Mercury. Nature Geoscience, 2016, 9, 273-276.	12.9	134
35	Characterization of artifacts introduced by the empirical volcano-scan atmospheric correction commonly applied to CRISM and OMEGA near-infrared spectra. Icarus, 2016, 269, 111-121.	2.5	16
36	Mars Reconnaissance Orbiter and Opportunity observations of the Burns formation: Crater hopping at Meridiani Planum. Journal of Geophysical Research E: Planets, 2015, 120, 429-451.	3.6	30

#	Article	IF	CITATIONS
37	Mercury's global color mosaic: An update from MESSENGER's orbital observations. Icarus, 2015, 257, 477-488.	2.5	27
38	Constraints on the abundance of carbon in near-surface materials on Mercury: Results from the MESSENGER Gamma-Ray Spectrometer. Planetary and Space Science, 2015, 108, 98-107.	1.7	57
39	Mineralogy, morphology and stratigraphy of the light-toned interior layered deposits at Juventae Chasma. Icarus, 2015, 251, 315-331.	2.5	23
40	Orbital multispectral mapping of Mercury with the MESSENGER Mercury Dual Imaging System: Evidence for the origins of plains units and low-reflectance material. Icarus, 2015, 254, 287-305.	2.5	95
41	Spectral evidence for hydrated salts in recurring slope lineae on Mars. Nature Geoscience, 2015, 8, 829-832.	12.9	513
42	Embedded clays and sulfates in Meridiani Planum, Mars. Icarus, 2015, 248, 269-288.	2.5	42
43	Stratigraphy of the Caloris basin, Mercury: Implications for volcanic history and basin impact melt. Icarus, 2015, 250, 413-429.	2.5	49
44	Phobos and Deimos. , 2015, , .		12
45	Recurring slope lineae in equatorial regions of Mars. Nature Geoscience, 2014, 7, 53-58.	12.9	248
46	Phase-ratio images of the surface of Mercury: Evidence for differences in sub-resolution texture. Icarus, 2014, 242, 142-148.	2.5	27
47	The value of Phobos sample return. Planetary and Space Science, 2014, 102, 176-182.	1.7	28
48	MERLIN: Mars-Moon Exploration, Reconnaissance and Landed Investigation. Acta Astronautica, 2014, 93, 475-482.	3.2	8
49	The low-iron, reduced surface of Mercury as seen in spectral reflectance by MESSENGER. Icarus, 2014, 228, 364-374.	2.5	82
50	Spectral absorptions on Phobos and Deimos in the visible/near infrared wavelengths and their compositional constraints. Icarus, 2014, 229, 196-205.	2.5	66
51	Ancient Aqueous Environments at Endeavour Crater, Mars. Science, 2014, 343, 1248097.	12.6	176
52	lmages of surface volatiles in Mercury's polar craters acquired by the MESSENGER spacecraft. Geology, 2014, 42, 1051-1054.	4.4	67
53	Composition of Surface Materials on the Moons of Mars. Planetary and Space Science, 2014, 102, 144-151.	1.7	40
54	MESSENGER at Mercury: Early orbital operations. Acta Astronautica, 2014, 93, 509-515.	3.2	4

#	Article	IF	CITATIONS
55	Mineral abundances at the final four curiosity study sites and implications for their formation. Icarus, 2014, 231, 65-76.	2.5	74
56	SciBox, an end-to-end automated science planning and commanding system. Acta Astronautica, 2014, 93, 490-496.	3.2	6
57	Mineralogy of the MSL Curiosity landing site in Gale crater as observed by MRO/CRISM. Geophysical Research Letters, 2014, 41, 4880-4887.	4.0	59
58	Global inventory and characterization of pyroclastic deposits on Mercury: New insights into pyroclastic activity from MESSENGER orbital data. Journal of Geophysical Research E: Planets, 2014, 119, 635-658.	3.6	79
59	Revised CRISM spectral parameters and summary products based on the currently detected mineral diversity on Mars. Journal of Geophysical Research E: Planets, 2014, 119, 1403-1431.	3.6	280
60	A hematite-bearing layer in Gale Crater, Mars: Mapping and implications for past aqueous conditions. Geology, 2013, 41, 1103-1106.	4.4	113
61	Automated processing of planetary hyperspectral datasets for the extraction of weak mineral signatures and applications to CRISM observations of hydrated silicates on Mars. Planetary and Space Science, 2013, 76, 53-67.	1.7	43
62	Prolonged magmatic activity on Mars inferred from the detection of felsic rocks. Nature Geoscience, 2013, 6, 1013-1017.	12.9	131
63	Craters hosting radarâ€bright deposits in Mercury's north polar region: Areas of persistent shadow determined from MESSENGER images. Journal of Geophysical Research E: Planets, 2013, 118, 26-36.	3.6	36
64	What the ancient phyllosilicates at Mawrth Vallis can tell us about possible habitability on early Mars. Planetary and Space Science, 2013, 86, 130-149.	1.7	99
65	First detection of Mars atmospheric hydroxyl: CRISM Near-IR measurement versus LMD GCM simulation of OH Meinel band emission in the Mars polar winter atmosphere. Icarus, 2013, 226, 272-281.	2.5	54
66	Mineralogy and morphology of geologic units at Libya Montes, Mars: Ancient aqueously derived outcrops, mafic flows, fluvial features, and impacts. Journal of Geophysical Research E: Planets, 2013, 118, 487-513.	3.6	56
67	Dark spots on Mercury: A distinctive lowâ€reflectance material and its relation to hollows. Journal of Geophysical Research E: Planets, 2013, 118, 1752-1765.	3.6	23
68	Spectral constraints on the formation mechanism of recurring slope lineae. Geophysical Research Letters, 2013, 40, 5621-5626.	4.0	33
69	Hydrous minerals on Mars as seen by the CRISM and OMEGA imaging spectrometers: Updated global view. Journal of Geophysical Research E: Planets, 2013, 118, 831-858.	3.6	420
70	Vertical distribution of dust and water ice aerosols from CRISM limbâ€geometry observations. Journal of Geophysical Research E: Planets, 2013, 118, 321-334.	3.6	74
71	The distribution and origin of smooth plains on Mercury. Journal of Geophysical Research E: Planets, 2013, 118, 891-907.	3.6	193
72	Insights into the subsurface structure of the Caloris basin, Mercury, from assessments of mechanical layering and changes in longâ€wavelength topography. Journal of Geophysical Research E: Planets, 2013, 118, 2030-2044.	3.6	37

#	Article	IF	CITATIONS
73	High spatial and temporal resolution sampling of Martian gas abundances from CRISM spectra. Journal of Geophysical Research E: Planets, 2013, 118, 89-104.	3.6	36
74	Hydrated minerals on Endeavour Crater's rim and interior, and surrounding plains: New insights from CRISM data. Geophysical Research Letters, 2012, 39, .	4.0	27
75	Areas of permanent shadow in Mercury's south polar region ascertained by MESSENGER orbital imaging. Geophysical Research Letters, 2012, 39, .	4.0	43
76	GETEMME—a mission to explore the Martian satellites and the fundamentals of solar system physics. Experimental Astronomy, 2012, 34, 243-271.	3.7	17
77	Extensive MRO CRISM observations of 1.27 <i>μ<</i> m O ₂ airglow in Mars polar night and their comparison to MRO MCS temperature profiles and LMD GCM simulations. Journal of Geophysical Research, 2012, 117, .	3.3	51
78	Compact Reconnaissance Imaging Spectrometer for Mars (CRISM) north polar springtime recession mapping: First 3 Mars years of observations. Journal of Geophysical Research, 2012, 117, .	3.3	39
79	Analysis of diskâ€resolved OMEGA and CRISM spectral observations of Phobos and Deimos. Journal of Geophysical Research, 2012, 117, .	3.3	52
80	A spectroscopic analysis of Martian crater central peaks: Formation of the ancient crust. Journal of Geophysical Research, 2012, 117, .	3.3	32
81	Most Mars minerals in a nutshell: Various alteration phases formed in a single environment in Noctis Labyrinthus. Journal of Geophysical Research, 2012, 117, .	3.3	74
82	The morphology of craters on Mercury: Results from MESSENGER flybys. Icarus, 2012, 219, 414-427.	2.5	53
83	Characterization of hydrated silicate-bearing outcrops in Tyrrhena Terra, Mars: Implications to the alteration history of Mars. Icarus, 2012, 219, 476-497.	2.5	42
84	Hollows on Mercury: MESSENGER Evidence for Geologically Recent Volatile-Related Activity. Science, 2011, 333, 1856-1859.	12.6	136
85	Columbus crater and other possible groundwater-fed paleolakes of Terra Sirenum, Mars. Journal of Geophysical Research, 2011, 116, .	3.3	148
86	New near-IR observations of mesospheric CO ₂ and H ₂ O clouds on Mars. Journal of Geophysical Research, 2011, 116, .	3.3	65
87	Subsurface water and clay mineral formation during the early history of Mars. Nature, 2011, 479, 53-60.	27.8	651
88	Flood Volcanism in the Northern High Latitudes of Mercury Revealed by MESSENGER. Science, 2011, 333, 1853-1856.	12.6	225
89	Journey to the Innermost Planet. Scientific American, 2011, 304, 34-39.	1.0	0
90	Eminescu impact structure: Insight into the transition from complex crater to peak-ring basin on Mercury. Planetary and Space Science, 2011, 59, 1949-1959.	1.7	19

#	Article	IF	CITATIONS
91	Photometric correction of Mercury's global color mosaic. Planetary and Space Science, 2011, 59, 1873-1887.	1.7	22
92	The global distribution of pyroclastic deposits on Mercury: The view from MESSENGER flybys 1–3. Planetary and Space Science, 2011, 59, 1895-1909.	1.7	105
93	Mercury's spectrophotometric properties: Update from the Mercury Dual Imaging System observations during the third MESSENGER flyby. Planetary and Space Science, 2011, 59, 1853-1872.	1.7	22
94	The transition from complex crater to peak-ring basin on Mercury: New observations from MESSENGER flyby data and constraints on basin formation models. Planetary and Space Science, 2011, 59, 1932-1948.	1.7	54
95	Evidence for low-grade metamorphism, hydrothermal alteration, and diagenesis on Mars from phyllosilicate mineral assemblages. Clays and Clay Minerals, 2011, 59, 359-377.	1.3	107
96	Seasonal Flows on Warm Martian Slopes. Science, 2011, 333, 740-743.	12.6	451
97	Stratigraphy, mineralogy, and origin of layered deposits inside Terby crater, Mars. Icarus, 2011, 211, 273-304.	2.5	131
98	Robust unmixing of hyperspectral images: Application to Mars. , 2011, , .		6
99	Whole-disk spectrophotometric properties of Mercury: Synthesis of MESSENGER and ground-based observations. Icarus, 2010, 209, 101-124.	2.5	35
100	Geomorphic knobs of Candor Chasma, Mars: New Mars Reconnaissance Orbiter data and comparisons to terrestrial analogs. Icarus, 2010, 205, 138-153.	2.5	26
101	Hydrated mineral stratigraphy of Ius Chasma, Valles Marineris. Icarus, 2010, 206, 253-268.	2.5	119
102	A Late Amazonian alteration layer related to local volcanism on Mars. Icarus, 2010, 207, 265-276.	2.5	39
103	Diagenetic haematite and sulfate assemblages in Valles Marineris. Icarus, 2010, 207, 659-674.	2.5	63
104	Exposure of spectrally distinct material by impact craters on Mercury: Implications for global stratigraphy. Icarus, 2010, 209, 210-223.	2.5	82
105	Silica deposits in the Nili Patera caldera on the Syrtis Major volcanic complex on Mars. Nature Geoscience, 2010, 3, 838-841.	12.9	173
106	Detection of Hydrated Silicates in Crustal Outcrops in the Northern Plains of Mars. Science, 2010, 328, 1682-1686.	12.6	134
107	Nearâ€ŧropical subsurface ice on Mars. Geophysical Research Letters, 2010, 37, .	4.0	79
108	Compact Reconnaissance Imaging Spectrometer for Mars (CRISM) south polar mapping: First Mars year of observations. Journal of Geophysical Research, 2010, 115, .	3.3	58

#	Article	IF	CITATIONS
109	Spectrally distinct ejecta in Syrtis Major, Mars: Evidence for environmental change at the Hesperianâ€Amazonian boundary. Journal of Geophysical Research, 2010, 115, .	3.3	23
110	Mineralogy and stratigraphy of phyllosilicateâ€bearing and dark mantling units in the greater Mawrth Vallis/west Arabia Terra area: Constraints on geological origin. Journal of Geophysical Research, 2010, 115, .	3.3	104
111	Stratigraphy of hydrated sulfates in the sedimentary deposits of Aram Chaos, Mars. Journal of Geophysical Research, 2010, 115, .	3.3	74
112	Spectral and stratigraphic mapping of hydrated sulfate and phyllosilicateâ€bearing deposits in northern Sinus Meridiani, Mars. Journal of Geophysical Research, 2010, 115, .	3.3	73
113	Investigation of an Argyre basin ring structure using Mars Reconnaissance Orbiter/Compact Reconnaissance Imaging Spectrometer for Mars. Journal of Geophysical Research, 2010, 115, .	3.3	25
114	Definitive evidence of Hesperian basalt in Acidalia and Chryse planitiae. Journal of Geophysical Research, 2010, 115, .	3.3	73
115	Geologic setting of serpentine deposits on Mars. Geophysical Research Letters, 2010, 37, .	4.0	299
116	Diverse aqueous environments on ancient Mars revealed in the southern highlands. Geology, 2009, 37, 1043-1046.	4.4	142
117	Distribution of Mid-Latitude Ground Ice on Mars from New Impact Craters. Science, 2009, 325, 1674-1676.	12.6	279
118	An improvement to the volcano-scan algorithm for atmospheric correction of CRISM and OMEGA spectral data. Planetary and Space Science, 2009, 57, 809-815.	1.7	166
119	The tectonics of Mercury: The view after MESSENGER's first flyby. Earth and Planetary Science Letters, 2009, 285, 283-296.	4.4	135
120	Volcanism on Mercury: Evidence from the first MESSENGER flyby for extrusive and explosive activity and the volcanic origin of plains. Earth and Planetary Science Letters, 2009, 285, 227-242.	4.4	135
121	Evidence for intrusive activity on Mercury from the first MESSENGER flyby. Earth and Planetary Science Letters, 2009, 285, 251-262.	4.4	67
122	Emplacement and tectonic deformation of smooth plains in the Caloris basin, Mercury. Earth and Planetary Science Letters, 2009, 285, 309-319.	4.4	53
123	Explosive volcanic eruptions on Mercury: Eruption conditions, magma volatile content, and implications for interior volatile abundances. Earth and Planetary Science Letters, 2009, 285, 263-271.	4.4	128
124	Caloris impact basin: Exterior geomorphology, stratigraphy, morphometry, radial sculpture, and smooth plains deposits. Earth and Planetary Science Letters, 2009, 285, 297-308.	4.4	84
125	Phyllosilicates and sulfates at Endeavour Crater, Meridiani Planum, Mars. Geophysical Research Letters, 2009, 36, .	4.0	88
126	Identification of hydrated silicate minerals on Mars using MROâ€CRISM: Geologic context near Nili Fossae and implications for aqueous alteration. Journal of Geophysical Research, 2009, 114, .	3.3	483

#	Article	IF	CITATIONS
127	A synthesis of Martian aqueous mineralogy after 1 Mars year of observations from the Mars Reconnaissance Orbiter. Journal of Geophysical Research, 2009, 114, .	3.3	445
128	Evidence for the origin of layered deposits in Candor Chasma, Mars, from mineral composition and hydrologic modeling. Journal of Geophysical Research, 2009, 114, .	3.3	159
129	Compact Reconnaissance Imaging Spectrometer for Mars investigation and data set from the Mars Reconnaissance Orbiter's primary science phase. Journal of Geophysical Research, 2009, 114, .	3.3	178
130	Compact Reconnaissance Imaging Spectrometer for Mars observations of northern Martian latitudes in summer. Journal of Geophysical Research, 2009, 114, .	3.3	24
131	Composition, Morphology, and Stratigraphy of Noachian Crust around the Isidis basin. Journal of Geophysical Research, 2009, 114, .	3.3	144
132	Mineralogy of Juventae Chasma: Sulfates in the lightâ€ŧoned mounds, mafic minerals in the bedrock, and hydrated silica and hydroxylated ferric sulfate on the plateau. Journal of Geophysical Research, 2009, 114, .	3.3	156
133	Testing evidence of recent hydration state change in sulfates on Mars. Journal of Geophysical Research, 2009, 114, .	3.3	78
134	Characterization of phyllosilicates observed in the central Mawrth Vallis region, Mars, their potential formational processes, and implications for past climate. Journal of Geophysical Research, 2009, 114, .	3.3	117
135	Wavelength dependence of dust aerosol single scattering albedo as observed by the Compact Reconnaissance Imaging Spectrometer. Journal of Geophysical Research, 2009, 114, .	3.3	196
136	Compact Reconnaissance Imaging Spectrometer observations of water vapor and carbon monoxide. Journal of Geophysical Research, 2009, 114, .	3.3	137
137	In-flight performance of MESSENGER's Mercury Dual Imaging System. Proceedings of SPIE, 2009, , .	0.8	22
138	Evolution of the Rembrandt Impact Basin on Mercury. Science, 2009, 324, 618-621.	12.6	46
139	The Evolution of Mercury's Crust: A Global Perspective from MESSENGER. Science, 2009, 324, 613-618.	12.6	194
140	New Horizons: Anticipated Scientific Investigations atÂtheÂPluto System. Space Science Reviews, 2008, 140, 93-127.	8.1	74
141	Hydrated silicate minerals on Mars observed by the Mars Reconnaissance Orbiter CRISM instrument. Nature, 2008, 454, 305-309.	27.8	630
142	Clay minerals in delta deposits and organic preservation potential on Mars. Nature Geoscience, 2008, 1, 355-358.	12.9	293
143	MRO/CRISM Retrieval of Surface Lambert Albedos for Multispectral Mapping of Mars With DISORT-Based Radiative Transfer Modeling: Phase 1—Using Historical Climatology for Temperatures, Aerosol Optical Depths, and Atmospheric Pressures. IEEE Transactions on Geoscience and Remote Sensing, 2008, 46, 4020-4040.	6.3	41

144 An Efficient Uplink Pipeline for the MRO CRISM Instrument. , 2008, , .

#	Article	IF	CITATIONS
145	Phyllosilicate and sulfateâ€hematite deposits within Miyamoto crater in southern Sinus Meridiani, Mars. Geophysical Research Letters, 2008, 35, .	4.0	63
146	Geomorphologic and mineralogic characterization of the northern plains of Mars at the Phoenix Mission candidate landing sites. Journal of Geophysical Research, 2008, 113, .	3.3	22
147	Spirit Mars Rover Mission to the Columbia Hills, Gusev Crater: Mission overview and selected results from the Cumberland Ridge to Home Plate. Journal of Geophysical Research, 2008, 113, .	3.3	99
148	Geology of the Caloris Basin, Mercury: A View from MESSENGER. Science, 2008, 321, 73-76.	12.6	140
149	Reflectance and Color Variations on Mercury: Regolith Processes and Compositional Heterogeneity. Science, 2008, 321, 66-69.	12.6	167
150	Opaline silica in young deposits on Mars. Geology, 2008, 36, 847.	4.4	303
151	Orbital Identification of Carbonate-Bearing Rocks on Mars. Science, 2008, 322, 1828-1832.	12.6	560
152	Spectroscopic Observations of Mercury's Surface Reflectance During MESSENGER's First Mercury Flyby. Science, 2008, 321, 62-65.	12.6	94
153	Volcanism on Mercury: Evidence from the First MESSENGER Flyby. Science, 2008, 321, 69-72.	12.6	169
154	Return to Mercury: A Global Perspective on MESSENGER's First Mercury Flyby. Science, 2008, 321, 59-62.	12.6	170
155	Phyllosilicate Diversity and Past Aqueous Activity Revealed at Mawrth Vallis, Mars. Science, 2008, 321, 830-833.	12.6	328
156	A Closer Look at Water-Related Geologic Activity on Mars. Science, 2007, 317, 1706-1709.	12.6	185
157	CRISM multispectral summary products: Parameterizing mineral diversity on Mars from reflectance. Journal of Geophysical Research, 2007, 112, .	3.3	304
158	Compact Reconnaissance Imaging Spectrometer for Mars (CRISM) on Mars Reconnaissance Orbiter (MRO). Journal of Geophysical Research, 2007, 112, .	3.3	796
159	Mineralogic constraints on sulfurâ€rich soils from Pancam spectra at Gusev crater, Mars. Geophysical Research Letters, 2007, 34, .	4.0	89
160	The Geology of Mercury: The View Prior to the MESSENGER Mission. Space Science Reviews, 2007, 131, 41-84.	8.1	31
161	The Mercury Dual Imaging System on the MESSENGER Spacecraft. Space Science Reviews, 2007, 131, 247-338.	8.1	242

162 The Mercury Dual Imaging System on the MESSENGER Spacecraft. , 2007, , 247-338.

#	Article	IF	CITATIONS
163	The Geology of Mercury: The View Prior to the MESSENGER Mission. , 2007, , 41-84.		0
164	The design of the compact reconnaissance imaging spectrometer for mars (crism) instrument. , 2006, , .		0
165	Compact reconnaissance imaging spectrometer for Mars (CRISM): characterization results for instrument and focal plane subsystems. , 2004, , .		2
166	The CONTOUR remote imager and spectrometer (CRISP). , 2004, 5163, 84.		0
167	CRISM (Compact Reconnaissance Imaging Spectrometer for Mars) on MRO (Mars Reconnaissance) Tj ETQq1 1 C).784314 r	gBT /Overloc
168	CONTOUR forward imager on the Comet Nucleus Tour mission. , 2004, , .		1
169	Selected configuration tradeoffs of contour optical instruments. Acta Astronautica, 2003, 52, 111-116.	3.2	2
170	The CONTOUR remote imager and spectrograph. Acta Astronautica, 2003, 52, 427-431.	3.2	0
171	Spectral properties and geologic processes on Eros from combined NEAR NIS and MSI data sets. Meteoritics and Planetary Science, 2003, 38, 1053-1077.	1.6	33
172	A model for formation of dust, soil, and rock coatings on Mars: Physical and chemical processes on the Martian surface. Journal of Geophysical Research, 2002, 107, 7-1-7-17.	3.3	64
173	The geology of 433 Eros. Meteoritics and Planetary Science, 2002, 37, 1651-1684.	1.6	142
174	Preliminary Remediation of Scattered Light in NEAR MSI Images. Icarus, 2002, 155, 244-252.	2.5	17
175	Inflight Calibration of the NEAR Multispectral Imager. Icarus, 2002, 155, 229-243.	2.5	20
176	Detection of Temperature-Dependent Spectral Variation on the Asteroid Eros and New Evidence for the Presence of an Olivine-Rich Silicate Assemblage. Icarus, 2002, 155, 181-188.	2.5	20
177	An Estimate of Eros's Porosity and Implications for Internal Structure. Icarus, 2002, 155, 94-103.	2.5	61
178	Near-IR Reflectance Spectroscopy of 433 Eros from the NIS Instrument on the NEAR Mission. Icarus, 2002, 155, 119-144.	2.5	70
179	Eros: Shape, Topography, and Slope Processes. Icarus, 2002, 155, 18-37.	2.5	154
180	Color Variations on Eros from NEAR Multispectral Imaging. Icarus, 2002, 155, 145-168.	2.5	78

#	Article	IF	CITATIONS
181	433 Eros Global Basemap from NEAR Shoemaker MSI Images. Icarus, 2002, 155, 38-50.	2.5	13
182	The NEAR shoemaker mission to asteroid 433 eros. Acta Astronautica, 2002, 51, 491-500.	3.2	44
183	Space weathering on Eros: Constraints from albedo and spectral measurements of Psyche crater. Meteoritics and Planetary Science, 2001, 36, 1617-1637.	1.6	89
184	Mineralogical interpretation of reflectance spectra of Eros from NEAR nearâ€infrared spectrometer low phase flyby. Meteoritics and Planetary Science, 2001, 36, 1711-1726.	1.6	45
185	The MESSENGER mission to Mercury: scientific objectives and implementation. Planetary and Space Science, 2001, 49, 1445-1465.	1.7	361
186	The MESSENGER mission to Mercury: scientific payload. Planetary and Space Science, 2001, 49, 1467-1479.	1.7	118
187	The landing of the NEAR-Shoemaker spacecraft on asteroid 433 Eros. Nature, 2001, 413, 390-393.	27.8	190
188	Shoemaker crater as the source of most ejecta blocks on the asteroid 433 Eros. Nature, 2001, 413, 394-396.	27.8	111
189	The nature of ponded deposits on Eros. Nature, 2001, 413, 396-400.	27.8	162
190	Laser Altimetry of Small-Scale Features on 433 Eros from NEAR-Shoemaker. Science, 2001, 292, 488-491.	12.6	38
191	Imaging of Small-Scale Features on 433 Eros from NEAR: Evidence for a Complex Regolith. Science, 2001, 292, 484-488.	12.6	147
192	NEAR Lightcurves of Asteroid 433 Eros. Icarus, 2000, 145, 641-644.	2.5	3
193	Near-Infrared Spectral Variations of Martian Surface Materials from ISM Imaging Spectrometer Data. Icarus, 2000, 147, 444-471.	2.5	81
194	In-Flight Calibration of the Near Earth Asteroid Rendezvous Mission's Near Infrared Spectrometer I. Initial Calibrations. Icarus, 2000, 148, 550-571.	2.5	11
195	NEAR at Eros: Imaging and Spectral Results. Science, 2000, 289, 2088-2097.	12.6	250
196	Mineralogic and compositional properties of Martian soil and dust: Results from Mars Pathfinder. Journal of Geophysical Research, 2000, 105, 1721-1755.	3.3	274
197	Inflight Calibration of the NEAR Multispectral Imager. Icarus, 1999, 140, 66-91.	2.5	35
198	NEAR Encounter with Asteroid 253 Mathilde: Overview. Icarus, 1999, 140, 3-16.	2.5	121

#	Article	IF	CITATIONS
199	Mathilde: Size, Shape, and Geology. Icarus, 1999, 140, 17-27.	2.5	86
200	NEAR Photometry of Asteroid 253 Mathilde. Icarus, 1999, 140, 53-65.	2.5	109
201	Imaging of Asteroid 433 Eros During NEAR's Flyby Reconnaissance. Science, 1999, 285, 562-564.	12.6	61
202	Preliminary results on photometric properties of materials at the Sagan Memorial Station, Mars. Journal of Geophysical Research, 1999, 104, 8809-8830.	3.3	71
203	Mars Pathfinder spectral measurements of Phobos and Deimos: Comparison with previous data. Journal of Geophysical Research, 1999, 104, 9069-9079.	3.3	47
204	Chemical, multispectral, and textural constraints on the composition and origin of rocks at the Mars Pathfinder landing site. Journal of Geophysical Research, 1999, 104, 8679-8715.	3.3	226
205	Overview of the Mars Pathfinder Mission: Launch through landing, surface operations, data sets, and science results. Journal of Geophysical Research, 1999, 104, 8523-8553.	3.3	121
206	Observations of Phobos, Deimos, and bright stars with the Imager for Mars Pathfinder. Journal of Geophysical Research, 1999, 104, 9055-9068.	3.3	34
207	Rocks at the Mars Pathfinder Landing Site. American Scientist, 1999, 87, 36.	0.1	4
208	An overview of the NEAR multispectral imager-near-infrared spectrometer investigation. Journal of Geophysical Research, 1997, 102, 23709-23727.	3.3	42
209	In situ compositions of Martian volcanics: Implications for the mantle. Journal of Geophysical Research, 1997, 102, 25605-25615.	3.3	97
210	Results from the Mars Pathfinder Camera. Science, 1997, 278, 1758-1765.	12.6	242
211	NEAR's Flyby of 253 Mathilde: Images of a C Asteroid. Science, 1997, 278, 2109-2114.	12.6	185
212	Near Infrared Spectrometer for the Near Earth Asteroid Rendezvous Mission. Space Science Reviews, 1997, 82, 101-167.	8.1	18
213	Multi-Spectral Imager on the Near Earth Asteroid Rendezvous Mission. Space Science Reviews, 1997, 82, 31-100.	8.1	24
214	Multi-Spectral Imager On the Near Earth Asteroid Rendezvous Mission. , 1997, , 31-100.		2
215	Near Infrared Spectrometer for the Near Earth Asteroid Rendezvous Mission. , 1997, , 101-167.		7
216	Spectral properties and rotational spectral heterogeneity of 433 Eros. Journal of Geophysical Research, 1996, 101, 2201-2214.	3.3	66

#	Article	IF	CITATIONS
217	Spectral Properties and Heterogeneity of Phobos from Measurements byPhobos 2. Icarus, 1996, 123, 63-86.	2.5	91
218	Mass spectrometer instrumentation for landers on small bodies and planetary moons. Acta Astronautica, 1996, 38, 377-384.	3.2	5
219	The Galileo Imaging Team plan for observing the satellites of Jupiter. Journal of Geophysical Research, 1995, 100, 18935.	3.3	32
220	Diagenetic layers in the upper walls of Valles Marineris, Mars: Evidence for drastic climate change since the mid-Hesperian. Journal of Geophysical Research, 1995, 100, 26339.	3.3	22
221	Galileo Photometry of Asteroid 951 Gaspra. Icarus, 1994, 107, 37-60.	2.5	117
222	The Geology of Gaspra. Icarus, 1994, 107, 61-71.	2.5	96
223	Martian Aerosols: Near-Infrared Spectral Properties and Effects on the Observation of the Surface. Icarus, 1994, 111, 317-337.	2.5	55
224	Spatial Variations in the Spectral Properties of Bright Regions on Mars. Icarus, 1993, 105, 454-468.	2.5	89
225	An Unusual Spectral Unit in West Candor Chasma: Evidence for Aqueous or Hydrothermal Alteration in the Martian Canyons. Icarus, 1993, 106, 380-391.	2.5	44
226	Galileo imaging observations of lunar maria and related deposits. Journal of Geophysical Research, 1993, 98, 17183-17205.	3.3	92
227	Crustal diversity of the moon: Compositional analyses of Galileo solid state imaging data. Journal of Geophysical Research, 1993, 98, 17127-17148.	3.3	85
228	Lunar impact basins: New data for the western limb and far side (Orientale and South Poleâ€Aitken) Tj ETQq0 0 (ΩrgBT /Ον	erlock 10 Tf 5
229	Galileo Encounter with 951 Gaspra: First Pictures of an Asteroid. Science, 1992, 257, 1647-1652.	12.6	193
230	Color heterogeneity of the surface of Phobos: Relationships to geologic features and comparison to meteorite analogs. Journal of Geophysical Research, 1991, 96, 5925-5945.	3.3	64
231	Preliminary assessment of Termoskan observations of Mars. Planetary and Space Science, 1991, 39, 237-265.	1.7	11
232	Results of TV imaging of phobos (experiment VSK-FREGAT). Planetary and Space Science, 1991, 39, 281-295.	1.7	38
233	A possible interpretation of bright features on the surface of Phobos. Planetary and Space Science, 1991, 39, 341-347.	1.7	13
234	Phobos: Spectrophotometry between 0.3 and 0.6 μm and IR-radiometry. Planetary and Space Science, 1991, 39, 311-326.	1.7	21

#	Article	IF	CITATIONS
235	Tectonic and volcanic evolution of dark terrain and its implications for the internal structure and evolution of Ganymede. Journal of Geophysical Research, 1990, 95, 10743-10768.	3.3	31
236	The tectonics of icy satellites. Advances in Space Research, 1990, 10, 173-182.	2.6	2
237	The geologic evolution of Ganymede and its implications for the origin of the Ganymede-Callisto "dichotomy― Advances in Space Research, 1990, 10, 183-186.	2.6	0
238	Crater densities and crater ages of different terrain types on Ganymede. Icarus, 1989, 81, 271-297.	2.5	19
239	Television observations of Phobos. Nature, 1989, 341, 585-587.	27.8	41
240	Possible breakup of dark terrain on Ganymede by largeâ€scale shear faulting. Journal of Geophysical Research, 1988, 93, 8795-8824.	3.3	33
241	Terrain types and localâ€ s cale stratigraphy of grooved terrain on Ganymede. Journal of Geophysical Research, 1986, 91, E222.	3.3	36
242	Global reorientation and its effect on tectonic patterns on Ganymede. Geophysical Research Letters, 1986, 13, 345-348.	4.0	15